*Brief Communication*

# Circadian rhythmic kinase CK2α phosphorylates BMAL1 to regulate the mammalian clock

Teruya Tamaru[1], Jun Hirayama[2], Yasushi Isojima[3], Katsuya Nagai[3], Shigemi Norioka[4], Ken Takamatsu[1] and Paolo Sassone-Corsi[2]

1 Department of Physiology, Toho University School of Medicine, 5-21-16 Ohmori-nishi Ohta-ku Tokyo 143-8540, Japan

2 Department of Pharmacology, School of Medicine, University of California, Irvine, California 92697, USA

3 Division of Protein Metabolism, Institute for Protein Research, Osaka University, 3-2 Yamadaoka, Suita, Osaka 565-0871, Japan

4 Division of Protein Chemistry, Institute for Protein Research, Osaka University, 3-2 Yamadaoka, Suita, Osaka 565-0871, Japan

Corresponding author: Paolo Sassone-Corsi,

Tel: 949 824 4540, Fax: 949 824 2078

E-mail: psc@uci.edu

**Clock proteins govern circadian physiology. We show that CK2α, corresponds to our previously reported kinase p45$^{PFK}$, rhythmically phosphorylates clock protein BMAL1 in the suprachiasmatic nuclei, the mammalian central pacemaker. Gene silencing for CK2α and BMAL1 mutagenesis of a CK2-phosphorylation site (Ser90) result in impaired nuclear BMAL1 accumulation and subsequent disruption of clock function. These findings reveal that circadian rhythmic kinase CK2 is an essential regulator of the mammalian circadian system.**



The circadian clock orchestrates intrinsic timing in most organisms and controls a large variety of physiological and metabolic programs[1]. The molecular core of the circadian clock is constituted by a number of gene products that operate in transcriptional-translational feedback loops[1, 2]. The BMAL1-CLOCK heterodimer is central to the clock mechanism by binding to promoter E-box elements, driving and maintaining circadian oscillations[3, 4]. A common feature of clock proteins in various organisms is their rhythmic phosphorylation[2, 5, 6]. Various kinases have been implicated, whereas the Drosophila dCK2 specifically regulates the nuclear entry of dPER thereby controlling the fly clock [7].

Periodically fluctuating kinases (PFKs) were originally described as clock-controlled enzymes in the rat suprachiasmatic nuclei (SCN) [8]. Purification and characterization of p45$^{PFK}$, the species displaying the highest fluctuation in enzymatic activity, indicated that it could function as a *bona fide* histone H1 and CLOCK kinase [8,9]. To establish the identity of p45$^{PFK}$, we performed a microsequencing analysis using Mass spectrometry (MS) on a highly gel-purified p45$^{PFK}$ from rat brain. The determined amino acid sequence revealed a complete match with rat CK2α (Supplementary Fig. 1). In a search of optimal clock targets for CK2α

(not shown), we found that purified $p45^{PFK}$ phosphorylates BMAL1 *in vitro* with the highest efficacy (Supplementary Fig. 2).

Based on these notions, we decided to explore whether CK2α would rhythmically phosphorylate BMAL1 in the SCN. To do so, we prepared CK2α-immunoprecipitates from both nuclear and cytoplasmic fractions isolated from rat SCN at various circadian times. The CK2α-immunoprecipitates were then used in kinase assays on BMAL1 as a substrate. A clear rhythmic pattern of BMAL1 phosphorylation is observed, particularly pronounced in the cytoplasmic fraction (Fig. 1A). Thus, CK2α functions as a circadian kinase, in accordance to the previously reported rhythmic activity of $p45^{PFK}$ [8]. On the other hand, the kinase function of the Drosophila CK2 toward a CK2-phosphorylation motif peptide does not display a rhythmic activity [7]. As the levels of all CK2 subunits in both nuclear and cytoplasmic fractions were basically constant during the circadian cycle (Fig. 1B), the subcellular distribution of the CK2 subunits is not likely to determine the rhythmic kinase activity in the SCN. Importantly, the peaks of CK2α-mediated phosphorylation of BMAL1 are at CT10 and CT22. These remarkably correlate with the circadian hyperphosphorylation of BMAL1 *in vivo* and with the accumulation of BMAL1 in the cytoplasm before nuclear entry (Fig. 1A and Supplementary Fig. 3). These findings suggest that CK2α-mediated rhythmic phosphorylation of BMAL1 determines its cyclic nuclear entry.

The physiological role of CK2α in the mammalian circadian clock was assessed by microRNAi (miR)-mediated silencing in dexamethazone (Dex)-treated NIH-3T3 fibroblasts. Using a specific miR-CK2α silencing vector with a transfection efficacy of about 40-60% (not shown) (Fig. 1C), CK2α expression was significantly reduced 48h post-transfection (Fig. 1C). To assess the effect of CK2α silencing on clock rhythmicity, we used a *mPer2*

promoter-driven luciferase reporter and monitored real time bioluminescence as previously reported [10]. Silencing of CK2α resulted in a drastic impairment of circadian *Per2* oscillation, as compared to cells transfected with the negative control-silencing vector (Fig. 1D). Indeed, after a first peak with significantly reduced *mPer2* expression, miR-CK2α transfected cells showed no subsequent circadian oscillation (Fig. 1D). The reason of this severe effect is likely to be ascribed to an aberrant BMAL1 intracellular localization. In fact, cells transfected with the control-silencing vector show a prominent nuclear localization of BMAL1 24h after Dex treatment, as expected [11]. Instead, silencing of CK2α results in a substantial retention of BMAL1 in the cytoplasm (Fig. 1E). These results are in keeping with the observation that, following cytoplasmic accumulation at ~16h, BMAL1 accumulates in the nucleus 20-24h after cells are Dex-treated (not shown) or serum-shocked [11]. Finally, treatment of serum-shocked cells with the CK2-specific inhibitor D-ribofuranosylbenzimidazole (DRB) caused cytoplasmic BMAL1 accumulation (Supplementary Fig. 4). This effect is circadian time-dependent, as it is observed only during the period when BMAL1 proteins, which have been accumulating in the cytoplasm, enter the nucleus (16-20h post serum-shock) [11]. As the function of the CLOCK-BMAL1 complex is totally dependent on the nuclear translocation of BMAL1[12], we reason that this is how CK2 exerts its control on the mammalian circadian clock. This role is reminiscent of the one observed in Drosophila by dCK2 in regulating the nuclear entry of dPER [7].

To establish the *in vivo* relevance of CK2α-mediated phosphorylation of BMAL1, we sought to identify the CK2 phosphoacceptor target site(s) in BMAL1 and determine its function in circadian rhythmicity. By MALDI-TOF/MS analysis we identified a likely phosphorylation site at position Ser90 (Fig. 2A). In this assay BMAL1 was highly phosphorylated at Ser90 by CK2α, while our results do not exclude the presence of other

minor phosphoacceptor site(s). Importantly, Ser90 is highly conserved among all vertebrate BMAL1s (Fig. 2B) and is embedded within an amino acid sequence that corresponds to a CK2 phosphorylation consensus site consisting of a Serine/Threonine residue with an acidic residue at the +3 position (S/T-X-X-D/E). Interestingly, while Ser90 is not conserved in the Drosophila counterpart of BMAL1, dCYCLE (not shown), consistent with the notion that dCK2α is unable of phosphorylating dCYCLE [7]. Thus, it would seem that the mode by which CK2 regulates the circadian machinery is different in mammals versus the fly. Finally, Ser90 is located near to the nuclear localization signal (NLS; Fig. 2B) [13], underscoring the possibility of a direct control of nucleocytoplasmic localization of BMAL1 by phosphorylation (see Fig. 1E).

Next, we wanted to establish the role of Ser90 phosphorylation in circadian function. To do so, we used mouse embryonic fibroblasts (MEFs) derived from *Bmal1*-null mice. Ablation of BMAL1 in these cells results in a dysfunctional circadian clock and arrhythmic gene expression [10,14]. Rescue experiments were performed by infecting *Bmal1*$^{-/-}$ MEFs with retroviruses expressing either wild-type BMAL1 (BMAL1-WT), a BMAL1-S90A mutant or GFP (Supplementary Fig. 5). Infected MEFs were synchronized by Dex treatment and circadian oscillation was monitored by a real-time bioluminescence assay using *mPer2* promoter-driven luciferase reporter vector. Infection of *Bmal1*$^{-/-}$ MEFs with a virus expressing BMAL1-WT rescued circadian *mPer2* expression, whereas the BMAL1-S90A mutant was unable to do so and generated lower *mPer2* expression. These results strongly suggest that BMAL1 phosphorylation by CK2α at Ser90 is essential for circadian gene expression (Fig. 2C).

Importantly, the ectopically expressed BMAL1-WT accumulated in the nucleus 24h after Dex treatment, an appropriate circadian time that reflects what normally occurs with native BMAL1 in NIH-3T3 cells and MEFs [11]. On the other hand, the BMAL1-S90A mutant remained mostly cytoplasmic (Fig. 2D). Similarly CLOCK, whose intracellular localization pattern matches BMAL1 [12], could not accumulate in the nucleus when coexpressed with BMAL1-S90A (not shown). These data nicely fit the change in the pattern of BMAL1 localization upon CK2α silencing (Fig. 1E), and stress the notion that circadian function requires phosphorylation of BMAL1 and its nuclear accumulation.

Our findings demonstrate that CK2α is a circadian rhythmic BMAL1 kinase that plays an essential role in the mammalian clock. CK2α-mediated phosphorylation of BMAL1 appears to constitute an important step for BMAL1 nuclear entry that timely follows its accumulation in the cytoplasm. Indeed, DRB-induced cytoplasmic BMAL1 retention occurs only during the period when cytoplasmic accumulated BMAL1 proteins normally enter the nucleus (Supplementary Fig. 4). While it is likely that CK2 influences circadian physiology at multiple levels because it phosphorylates a large array of cellular proteins [15], the remarkable specificity observed here on BMAL1-Ser90 provides a lead to further investigations. Finally, as BMAL1 has been recently shown to be SUMOylated and acetylated [10,14], we believe that the regulatory pathway presented here constitutes a valuable gateway to future investigations aimed at unraveling the interplay between phosphorylation and other post-translational modifications of clock proteins.

**Acknowledgements.** We thank M. Okada and T. Takao (Osaka University, Japan) for MS analysis, E.G. Krebs, L. Dongxia (University of Washington, USA), J. S. Takahashi (Northwestern University, USA), C.A. Bradfield (University of Wisconsin, USA), S.M. Reppert (Harvard University, USA), M. Ikeda (Saitama Medical University, Japan) and C. Nishio (Osaka University, Japan) and members of Sassone-Corsi laboratory for kind sharing of reagents, discussions and help. This work was supported by the Human Frontiers Science Program Organization and Japanese MECSST (T. T. and K. T.) and by the Cancer Research Coordinating Committee of the University of California and from the National Institute of Health (P. S.-C.).

**Refferences**

1. Reppert, S.M. & Weaver, D.R. *Nature* **418**, 935-941 (2002).

2. Harms, E., Kivimae, S., Young, M.W., & Saez, L. *J Biol Rhythms*. **19**, 361-73 (2004).

3. Gekakis, N., Staknis, D., Nguyen, H.B., Davis, F.C., Wilsbacher, L.D. *et al. Science* **280**, 1564-1569 (1998).

4. Bunger, M.K., Wilsbacher, L.D., Moran, S.M., Cledenin, C., Radcriffe, L.A. *et al. Cell* **103**, 1009-1017 (2000).

5. Edery, I., Zwiebel, L. J., Dembiska, M. E. & Rosbash, M. *Proc. Nat. Acad. Sci. US.A.* **91**, 2260-2264 (1994).

6. Lee, C., Etchegaray, J.P., Cagampang, F.R.A., Loudon, S.I. & Reppert, S.M. Cell 107, 855-867 (2001).

7. Lin, J.M., Kilman, V.L., Keegan, K., Paddock, B., Emery-Le., M, Rosbash, M. *et al. Nature*. **420**, 816-20 (2002).

8. Tamaru, T., Okada, M., Nagai, K., Nakagawa, H. & Takamatsu, K. *J. Neurochem.* **72**, 2191-2197 (1999).

9. Tamaru, T., & Okada, M. *Eur J Biochem*. **238**, 152-159 (1996).

10. Hirayama, J., Sahar, S., Grimaldi, B., Tamaru, T., Takamatsu, K. *et al. Nature* **450**, 1086-1090 (2007).

11. Tamaru T., Isojima Y., van der Horst G.T.J., Takei K., Nagai K. *et al. Genes Cells* **8**, 973-983 (2003).

12. Kondratov, R.V., Chernov M.V., Kondratova A. A., Gorbacheva V.Y., Gudkov A.V. *et al. Genes and Dev.* **17**, 1921-1932 (2003).

13. Kwoon, I., Lee ,J., Chan, S.K., Jung, N.C., Lee, B.J. *et al. Mol.Cell. Biol.* **26**, 7318-7370 (2006).

14. Cardone, L., Hirayama, J., Giordano, F., Tamaru, T., Palvimo, J. *et al. Science* **309**, 1390-1394 (2005).

15. Meggio, F., & Pinna, L.A. *FASEB J.* **17**, 349-68 (2003).

## Figure Legends

### Figure 1

**Circadian rhythmic kinase CK2α is a mammalian clock component that controls BMAL1 nuclear entry.**

**A)** Nuclear (N) and cytoplasmic (C) fractions of rat SCN from each circadian time (n=8) were subjected to CK2α-immunoprecipitation for BMAL1 kinase assay and immunoblotting. Arrows designate nonphosphorylated forms while bars designate phosphorylated forms. **B)** Immunoblotting for the CK2 subunits. **C)** NIH-3T3 cells expressing *mPer2* promoter-luciferase reporter were transfected (TF) with microRNAi (miR) targeting vector and the negative control vector, then treated with dexametazone (Dex). Lysates were subjected to immunoblotting. **D)** *mPer2* promoter activities were monitored by a real time bioluminescence assay. **E)** The miR-transfected GFP-positive cells at 24h post Dex treatment were stained with anti-BMAL1. Nuclei were stained with DAPI. The values of nuclear BMAL1-dominant cells in the GFP-positive cells are plotted as means ± SEM. (***; $P < 0.001$).



### Figure 2

**The Ser90 CK2 phosphorylation site in BMAL1 is essential for circadian rhythmicity and controls BMAL1 nuclear entry.**

**A)** BMAL1 phosphorylation site(s) by CK2α was determined by MALDI-Tof/MS analysis. The arrow indicates the peak corresponding to Ser90-phosphorylation. **B)** The sequence alignment of BMAL1 around the CK2α-phosphorylation target Ser from various species is shown. **C)** *mPer2* promoter activities of *Bmal1*$^{-/-}$ MEFs expressing Myc-BMAL1-WT (wild

type), Myc-BMAL1-S90A (Ser90-deficient mutant) and Myc-GFP (control) were monitored by a real time bioluminescence assay. D) MEFs at 24h post Dex treatment were stained with anti-BMAL1 antibody. Nuclei were stained with DAPI. The values of nuclear BMAL1-dominant cells are plotted as means $\pm$ SEM (***; $P < 0.001$).

(Supplementary figure legends)

**S 1. Circadian periodically fluctuating kinase, p45$^{PFK}$ is CK2α.**

**A:** The 2D-gel electrophoresis pattern for purified p45$^{PFK}$. p45$^{PFK}$ was purified as described previously [9]. The concentrated samples were subjected to 2D-electrphoresis with or without Histone H1 in the SDSPAGE-gel. The Histone H1-containing gel was subjected to in gel kinase assay. The gel was subjected to silver staining. The gel containing Histone H1 phosphorylating activity (surrounded in the figure) was excised for the microsequencing analysis using Mass spectrometry. **B:** Amino acid sequences of rat, human and Drosophila CK2α. Deduced amino acid sequences by MS analysis are shown as red-colored letters.

**S 2. Purified p45$^{PFK}$ phosphorylates BMAL1.**

Purified p45$^{PFK}$ was subjected to *in vitro* kinase assay using GST-BMAL1 as a substrate. Proteins were resolved on SDS-PAGE, and the gels were visualized with CBB-staining and autoradiography. Purified p45$^{PFK}$ did not phosphorylate GST, as shown previously [9].

**S 3. Phosphorylation of BMAL1 protein in the rat SCN.**

Rat SCN from CT10 (n=4) was separated into nuclear (Nucleus) and cytoplasmic (Cytoplasm) fractions. +λPPase; aliquots of the samples (20 μg protein) were treated with λ protein phosphatase, and then subjected to immunoblot analysis using anti-BMAL1 antibody. The phosphorylated (bar) and unphosphorylated (arrow) forms of proteins are indicated.

**S 4. Circadian time dependent suppression of BMAL1 nuclear entry by CK2 inhibitor.**

Serum shocked NIH-3T3 cells were treated with CK2 inhibitor (20 μM DRB) and control (DMSO) at 12-16h, 16-20h and 26-30h post serum shock. The cells were immunocytochemically stained with anti-BMAL1 (Green). Nuclei were stained with DAPI (Blue).

**S5. Equivalent levels of ectopically expressed BMAL1 proteins in MEFs.**

Total cell extracts from MEFs stably expressing *mBmal1* promoter-driven Myc-BMAL1-WT, Myc-BMAL1-S90A (CK2 major phosphorylation site-deficient mutant) and CMV-promoter-driven Myc-GFP (as control) were subjected to immunoblot analysis detected by anti-Myc antibody.

***Supplementary methods***

**Kinase assay, immunoprecipitation, immunoblot and immunocytochemistry**

In gel and *in vitro* kinase assay were performed as described previously [8], using redivue [γ-$^{32}$P] ATP (Amersham, Japan). Kinase activities were visualized as artificial colors showing the intensity as a red to blue color gradient with red as higher intensity, which was analyzed with a BAS2000 imager (Fuiji film). Histone-H1 (Boehringer Mannheim, Japan), purified p45$^{PFK}$ [9], CK2α, Sf9 cells-produced GST-mBMAL1 (full-length) was prepared according to the manufacturer's protocol (Baculo Gold transfection system; Pharmingen, USA), E-Coli produced GST and GST-mBMAL1 were prepared as described previously [9]. CK2α was prepared by excising CK2α portion from GST-CK2α using Precision protease (Amersham, Japan).

Immunoprecipitation (using 100μg protein from the rat SCN), immunoblot (using 10μg protein) and immunocytochemistry were performed as described previously [11], using anti-BMAL1 [11], Histone H1, Actin (Santa Cruz. Biotech., USA), Myc-tag (Upstate Biotechnology, USA), HRP-conjugated anti-rabbit IgG (Zymed, USA), Alexa Fluor 564/488-conjugated anti-rabbit IgG and DAPI (Molecular probes, USA). Our previously produced anti-BMAL1 antibody [11] detected BMAL1-immunoreactivity specifically in BMAL1-expressed cells whereas not in mouse embryonic fibroblasts from *Bmal1*-null mice (*Bmal1*$^{-/-}$ MEFs) (data not shown).

**Microsequencing and determination of the phosphorylation site**

Purification of $p45^{PFK}$ from rat brain was performed as described previously [9]. The concentrated samples were subjected to 2D-electrphoresis with or without Histone H1 in the SDSPAGE-gel. The Hisotne H1-containing gel was subjected to in gel kinase assay as described previously [8]. Another gel was subjected to silver staining. The gel portion containing Histone H1 phosphorylating activity (surrounded in Supplementary Fig. 1) was excised for the microsequencing analysis using Mass spectrometry (MS).

GST-mBMAL1 was purified from E.coli, BL21 (Amercham, JAPAN) transformed with pGEX-6P-mBMAL1b (full length), which was kindly donated by Chika Nishio (Osaka University). GST-mBMAL1 (75pmol) was phosphorylated by CK2α (37.5pmol) after alkaline phosphatase treatment. This reaction was performed under the optimal kinase:substrate ratio, which was pre-determined (data not shown). BMAL1 phosphorylation site by CK2α was determined by MALDI-Tof/MS analysis using Voyager System according to the manufacturer's protocol (Applied Biosystems, JAPAN).

**Preparation of the SCN extracts** Male Wistar rats aged 5-8 weeks were were maintained at 25 $^{o}$C on a 12 h light and 12 h dark cycle for at least 1 week before use. Animals were decapitated at each experimental circadian time (CT) point. The SCN region was punched out with a 2mm-diameter needle as described previously [8]. Nuclear and cytoplasmic fractions at the indicated time points were prepared as described previously [8].

**Plasmid construction**

The vector, pcDNA6.3-GW/EmGFP-miR-CK2α for gene silencing study with microRNAi for mouse CK2α knock down was constructed according to the manufacturer's protocol (Invitrogene, JAPAN) using following target sequence.

Top strand;

5'-TGCTGTTCTGTTCCCAGAACCTTGGCGTTTTGGCCACTGACTGACGCC AAGGTTGGGAACAGAA -3'

Bottom Strand;

5'-CCTGTTCTGTTCCCAACCTTGGCGTCAGTCAGTGGCCAAAACGCCAAGGTTCT GGGAACAGAAC -3'

The vector, pGL4-Per2, was constructed to express 1.7kb *mPer2* promoter–driven destabilized luciferase reporter. E.coli expression vector for GST-CK2α was constructed by inserting of PCR products of full-length hCK2α ORF to the C-terminal of GST sequence in pGEX-6p vector (Amersham, Japan).

Retroviral expression vector (pCLNCX) for *Bmal1* promoter-driven Myc-BMAL1 was generated as previously described [10,14]. The CK2 major phosphorylation site-deficient BMAL1 mutant, S90A was generated with exchanging Ser90 to Ala in mBMAL1b by using the QuickChange site-directed mutagenesis (Stratagene, USA).

**Cell culture, transfection and retroviral infection**

NIH-3T3 cells and MEFs were cultured as described previously [11]. For clock synchronization, cells were treated with 0.1μM Dexamethazone for 2h. DNA transfection was performed using Fugene 6 and Fugene HD (Roche, Japan) according to the manufacturer's protocol. RetroMax expression system (IMGENEX, USA) was used to produce retrovirus according to manufacturer's protocol. For infection, *Bmal1*$^{-/-}$ MEFs, which is kindly donated by

Christopher A. Bradfield (University of Wisconsin, USA), were incubated with viral solution for 3h and this procedure was repeated 4 times. As the results, nearly 100% *Bmal1*$^{-/-}$ MEFs was rescued with *mBmal1* promoter-driven Myc-BMAL1 wild type and the mutant (S90A) or CMV-promoter-driven Myc-GFP as the negative control.

**Real-time bioluminescence assay**

Cells were transfected with plasmids in 10% FBS/DMEM on 35mm dishes. 24h after the transfection, cells were treated with 0.1μM Dexamethazone for 2h. Real time bioluminescence activities were monitored using Kronos (ATTO, Japan) after changing medium to 20%FBS/DMEM containing 0.1mM Luciferin and 25mM Hepes, pH7.2.

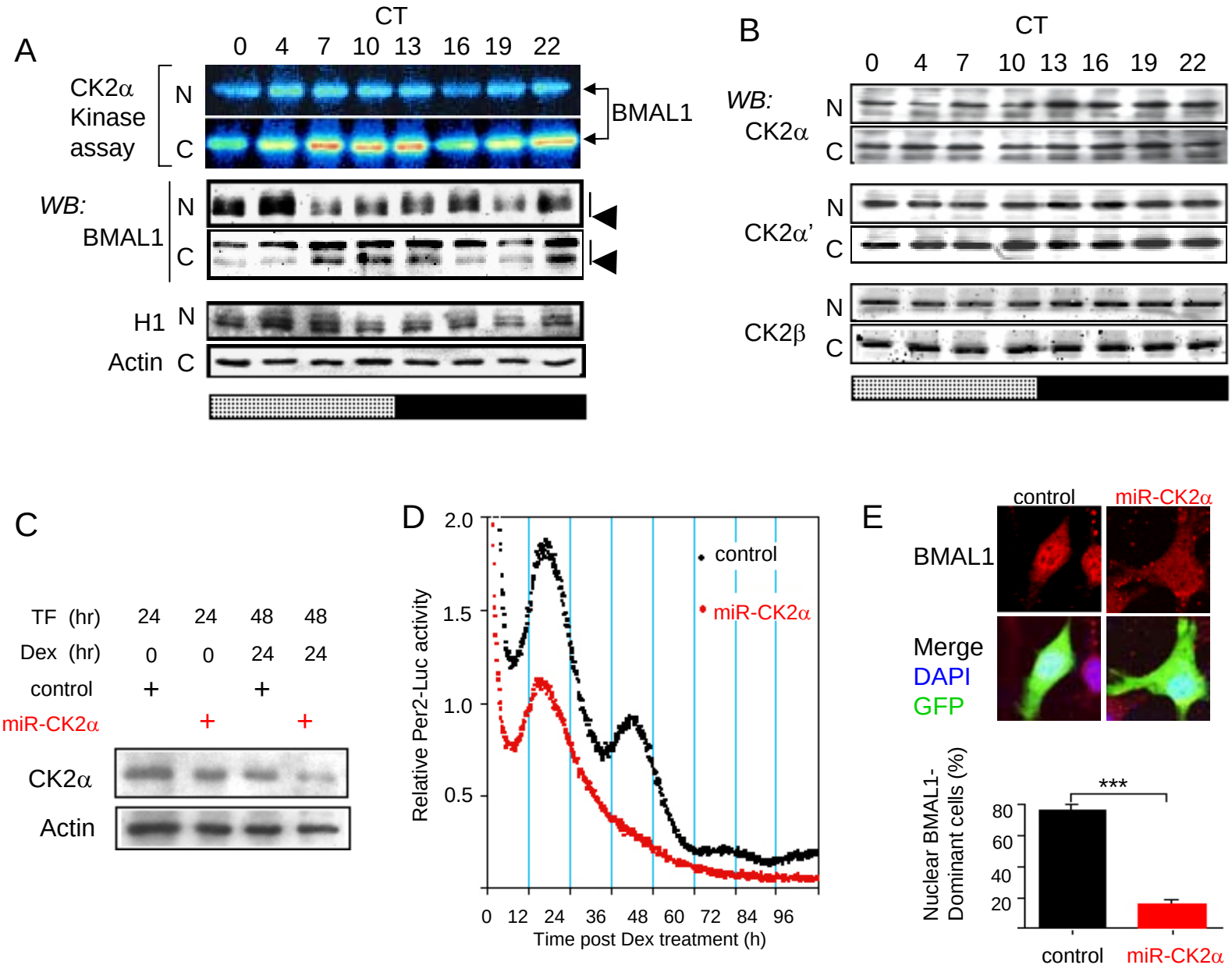


Figure-1 Sassone-Corsi.

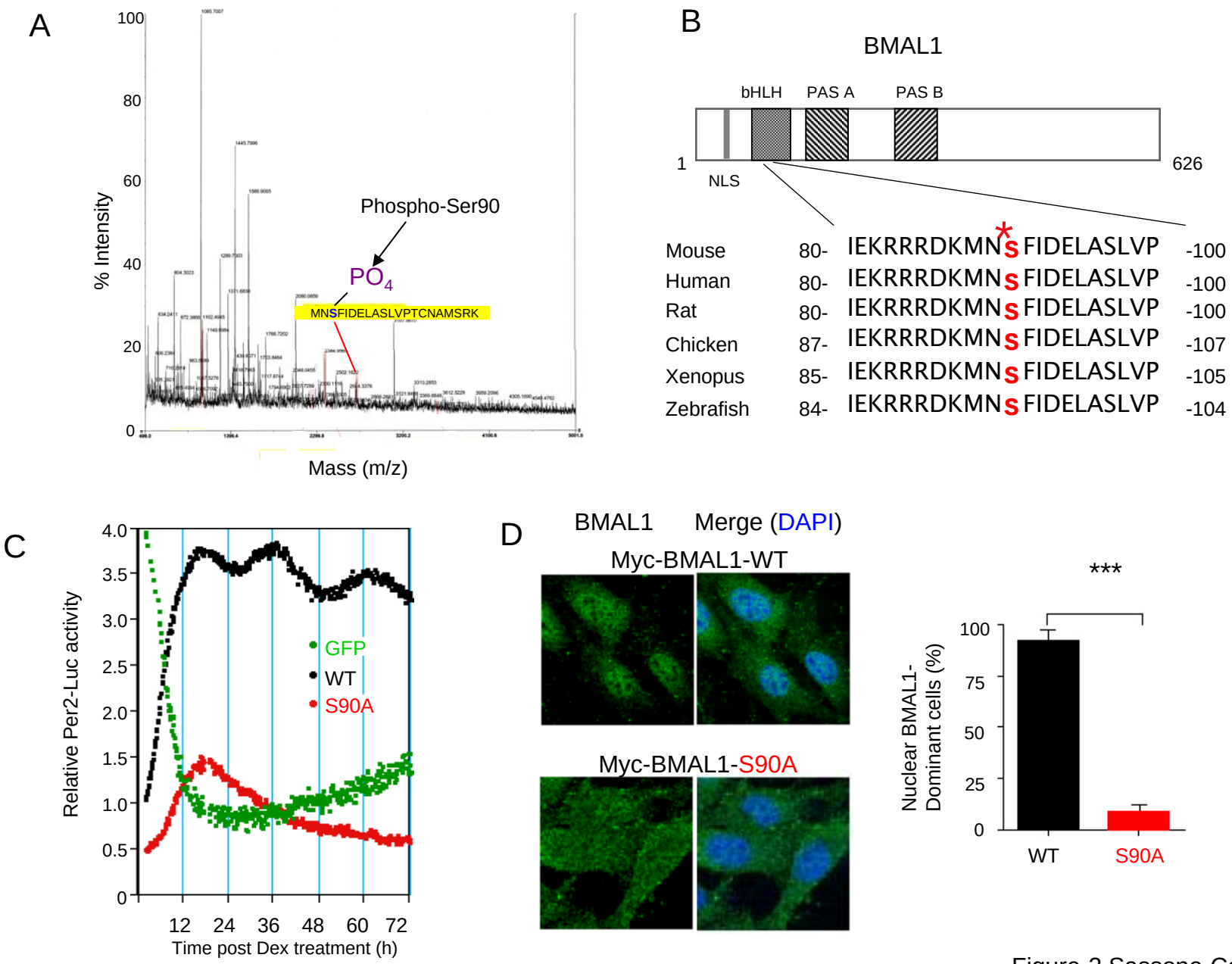


Figure-2 Sassone-Corsi.

A

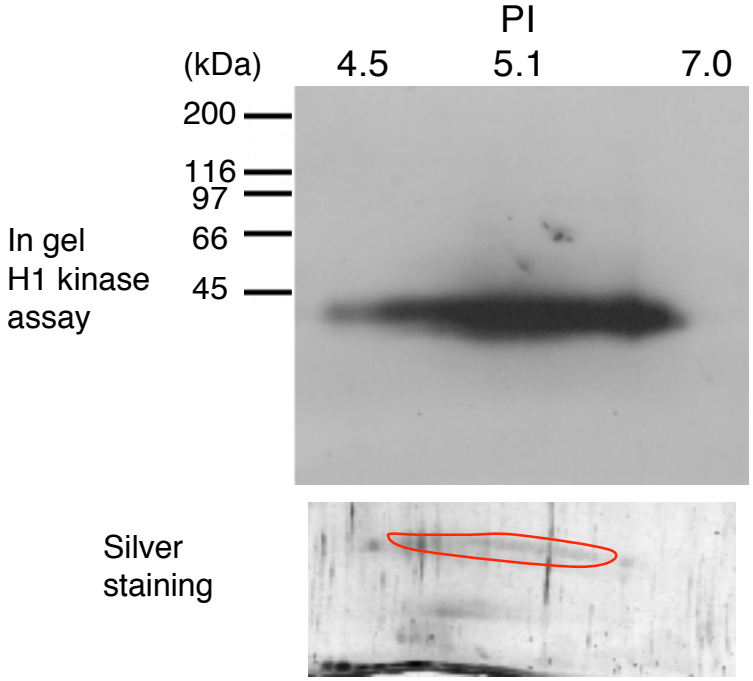


B

```
                1       10        20        30        40        50        60        70
rCK2α    MSGPVPSRARVYTDVNTHRPREYWDYESHVVEWGNQDDYQLVRKLGRGKYSEVFEAINITNNEKVVVKIL
         ************************************************************************
hCK2α    MSGPVPSRARVYTDVNTHRPREYWDYESHVVEWGNQDDYQLVRKLGRGKYSEVFEAINITNNEKVVVKIL
              ** ******** * * ******  ** ****************************  ** *****
dCK2α      MTLPSAARVYTDVNAHKPDEYWDYENYVVDWGNQDDYQLVRKLGRGKYSEVFEAINITTTEKCVVKIL

                71        80        90       100       110       120       130       140
         KPVKKKKIKREIKILENLRGGPNIITLADIVKDPVSRTPALVFEHVNNTDFKQLYQTLTDYDIRFYMYEI
         ************************************************************************
         KPVKKKKIKREIKILENLRGGPNIITLADIVKDPVSRTPALVFEHVNNTDFKQLYQTLTDYDIRFYMYEI
         ******************** *****   *********** ****************** ** *  *
         KPVKKKKIKREIKILENLRGGTNIITLLAVVKDPVSRTPALIFEHVNNTDFKQLYQTLTDYEIRYYLFEL

                141       150       160       170       180       190       200       210
         LKALDYCHSMGIMHRDVKPHNVMIDHEHRKLRLIDWGLAEFYHPGQEYNVRVASRYFKGPELLVDYQMYD
         ************************************************************************
         LKALDYCHSMGIMHRDVKPHNVMIDHEHRKLRLIDWGLAEFYHPGQEYNVRVASRYFKGPELLVDYQMYD
         ************************** ****************************************
         LKALDYCHSMGIMHRDVKPHNVMIDHENRKLRLIDWGLAEFYHPGQEYNVRVASRYFKGPELLVDYQMYD

                211       220       230       240       250       260       270       280
         YSLDMWSLGCMLASMIFRKEPFFHGHDNYDQLVRIAKVLGTEDLYDYIDKYNIELDPRFNDILGRHSRKR
         ************************************************************************
         YSLDMWSLGCMLASMIFRKEPFFHGHDNYDQLVRIAKVLGTEDLYDYIDKYNIELDPRFNDILGRHSRKR
         ************************************** ** * ***** ***** *** ******
         YSLDMWSLGCMLASMIFRKEPFFHGHDNYDQLVRIAKVLGTEELYAYLDKYNIDLDPRFHDILQRHSRKR

                281       290       300       310       320       330       340       350
         WERFVHSENQHLVSPEALDFLDKLLRYDHQSRLTAREAMEHPYFYTVVKDQARMSSAGMAGGSTPVSSAN
         ************************************************** *  * **********
         WERFVHSENQHLVSPEALDFLDKLLRYDHQSRLTAREAMEHPYFYTVVKDQARMGSSSMPGGSTPVSSAN
         ******* ********************  ******** ****   *  *
         WERFVHSDNQHLVSPEALDFLDKLLRYDHVDRLTAREAMAHPYFLPIVNGQMNPNNQQ
```

Supplementary Figure-1 Sassone-Corsi

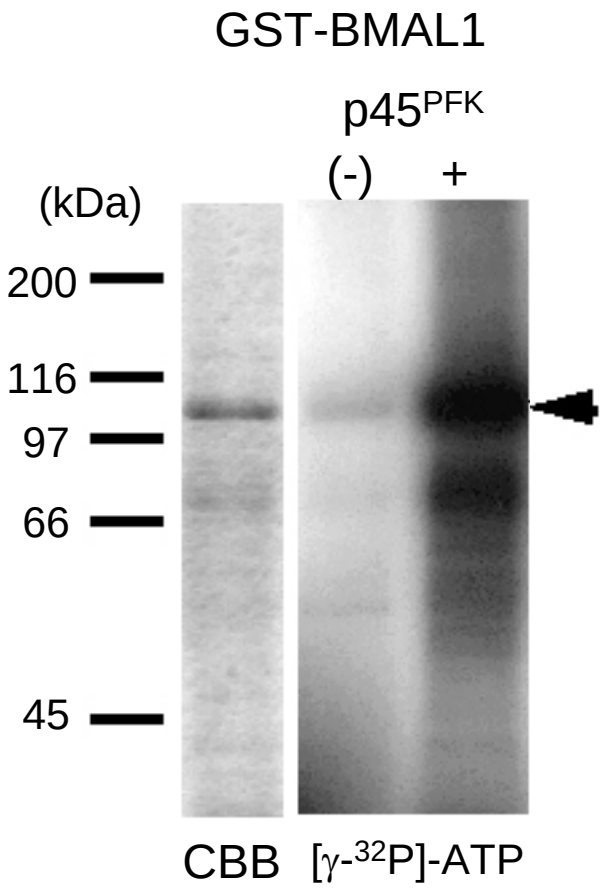


Supplementary Figure-2 Sassone-Corsi

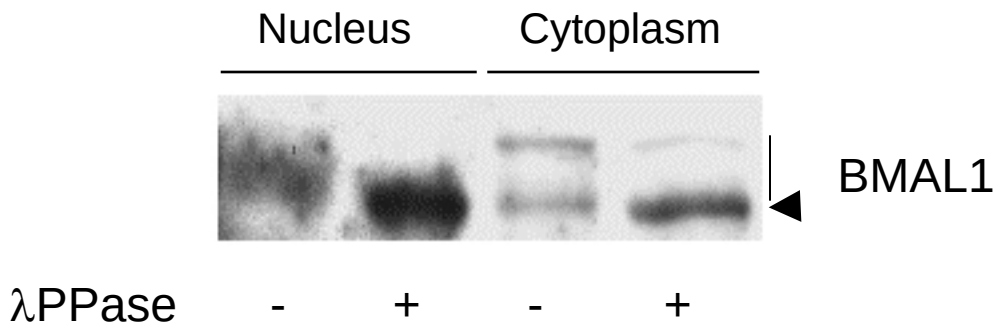


Supplementary Figure-3 Sassone-Corsi

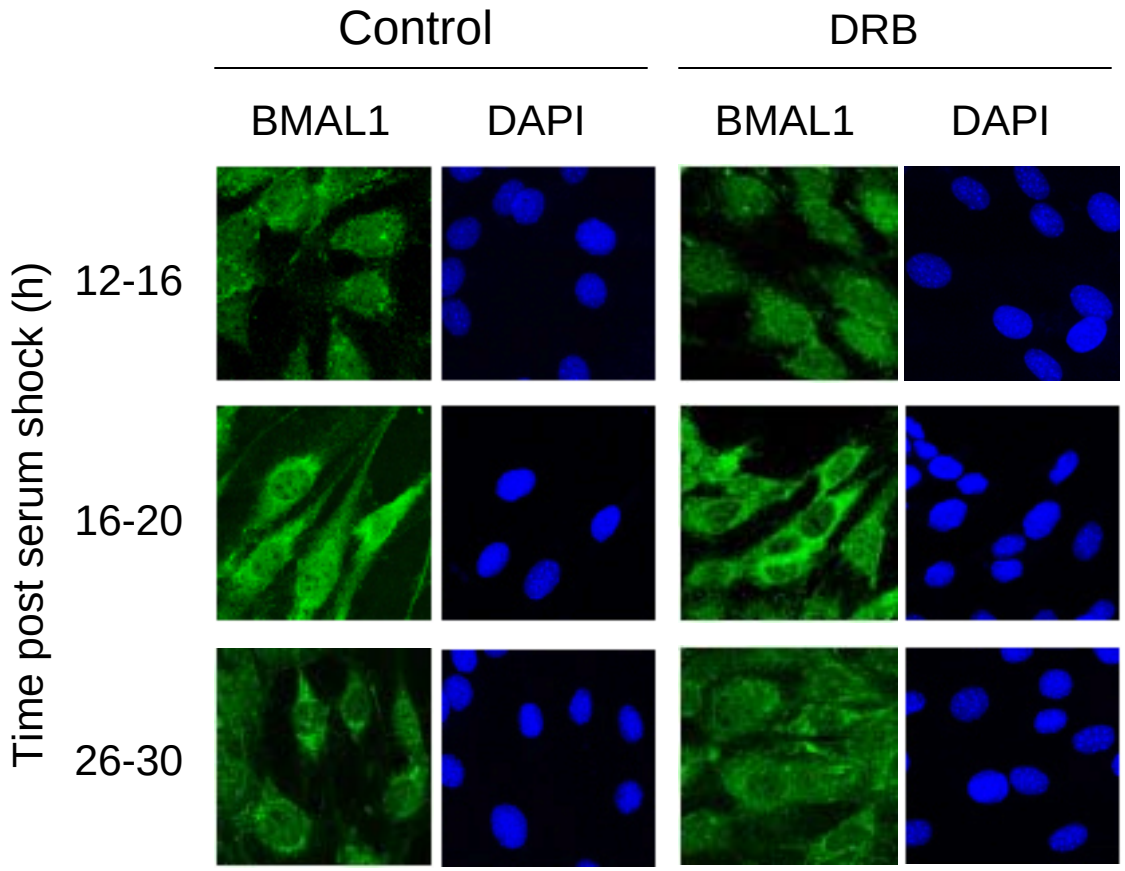


Supplementary Figure-4 Sassone-Corsi

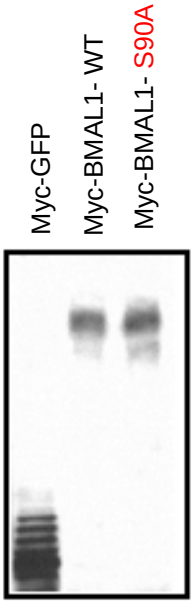


Supplementary Figure- 5 Sassone-Corsi